JOURNAL OF VIROLOGY, June 2003, p. 7041–7047 Vol. 77, No. 12
0022-538X/03/$08.00+0 DOI: 10.1128/JVI.77.12.7041–7047.2003

Interactions of Rotavirus VP4 Spike Protein with the Endosomal Protein Rab5 and the Prenylated Rab Acceptor PRA1

Vincent Enouf,[1] Serge Chwetzoff,[2] Germain Trugnan,[2] and Jean Cohen[1]*

Virologie Moléculaire et Structurale, UMR CNRS-INRA 2472, F-91190 Gif-sur-Yvette,[1] and INSERM U538, Faculté de Médecine Saint-Antoine, 75012 Paris,[2] France

Received 17 September 2002/Accepted 27 March 2003

Rotavirus spike protein VP4 is implicated in several important functions, such as cell attachment, penetration, hemagglutination, neutralization, virulence, and host range. It is present at the plasma membrane and colocalizes with the cytoskeleton in infected cells. We looked for cellular partners responsible for the localization of VP4 by two-hybrid screening of a monkey CV1 cell cDNA library. In the screen we isolated repeatedly three cDNAs encoding either two isoforms (a and c) of Rab5 protein or the prenylated Rab acceptor (PRA1). The small GTPase Rab5 is a molecule regulating the vesicular traffic and the motility of early endosomes along microtubules. Rab5 interacts with a large number of effectors, in particular with PRA1. Interactions of VP4 with both partners, Rab5 and PRA1, were confirmed by coimmunoprecipitation from infected- or transfected-cell lysates. Interaction of Rab5 and PRA1 was restricted to free VP4, since neither triple-layered particles nor NSP4-VP4-VP7 heterotrimeric complexes could be coprecipitated. Site-directed and deletion mutants of VP4 were used to map a VP4 domain(s) interacting with Rab5 or PRA1. Of the 10 mutants tested, 2 interacted exclusively with a single partner. In contrast, the domain extending from amino acids 560 to 722 of VP4 is essential for both interactions. These results suggest that Rab5 and PRA1 may be involved in the localization and trafficking of VP4 in infected cells.

Rotaviruses are the leading cause of severe gastroenteritis in young children worldwide (24). Structural and biochemical analyses show that rotaviruses are large, icosahedral particles consisting of three concentric capsid layers surrounding a genome of 11 segments of double-stranded RNA (15, 45). VP4 is a nonglycosylated protein and forms spikes that project from the rotavirus surface. Trypsin cleavage of VP4 into the fragments VP8* and VP5* is required for viral infectivity and stabilization of the spikes (11, 30). VP4 has been implicated in several important functions, such as cell attachment, penetration, hemagglutination, neutralization, and virulence (10, 17, 26, 32). It has been shown previously that VP5*, which includes a conserved hydrophobic region located between amino acids (aa) 384 and 401 of VP4, is a specific membrane-permeabilizing protein and could play a role in the cellular entry of rotaviruses (12). Heterotrimers consisting of VP4, NSP4, and VP7 may participate in the budding of the single-shelled particles into the lumen of the endoplasmic reticulum, where maturation to double-shelled particles seems to occur (33, 39).

Rab proteins are a family of Ras-related low-molecular-weight monomeric GTP-binding proteins (~20 to 29 kDa) which are key regulators of vesicular transport within eukaryotic cells (7). Several effector proteins alter either the state of phosphorylation or the intracytoplasmic location of Rab proteins and thus modulate their biological activity (25). The first modification refers to a posttranslational covalent addition of two 20-carbon isoprenoid geranyl-geranyl groups to free cysteine residues near or at the carboxy terminus (2). Isoprenylation facilitates association of Rab proteins with membrane-bound compartments and allows their localization to the cytoplasmic surface of distinct exocytic and endocytic organelles. The second modification refers to the state of phosphorylation. The GTPase-activating protein facilitates the hydrolysis of GTP by the intrinsic GTPase activity of the Rab protein (7). The GDP-bound Rab is then released from membranes to the cytosol by the cytosolic Rab GDP dissociation inhibitor (GDI) (44). Conversely, the exchange of GDP for GTP is facilitated by the guanine nucleotide exchange factor, which favors Rab's return to membranes and prevents the displacement by Rab GDI. Another effector antagonizes the action of the GDI: the prenylated Rab acceptor (PRA). PRA favors the retention of Rab in the membrane by inhibiting its removal from the GDI (1). By means of these effectors favoring the transitions between states, Rab proteins can cycle between (i) an active GTP-bound form localized at the cytoplasmic side of different subcellular organelles and (ii) an inactive cytosolic GDP-bound form. Rab5 regulates the endocytic pathway and is an important component of the docking and fusion apparatus (19, 29). Three different Rab5 isoforms, Rab5a, -b, and -c, have been reported previously, but no differences in their functions in endocytosis have been discovered (9). In addition, Rab5 has also been shown elsewhere to regulate the motility of early endosomes along microtubules (38) and the formation of clathrin-coated vesicles at the plasma membrane (35).

In the present study, we have searched for intracellular partners of VP4. Using two-hybrid and coimmunoprecipitation experiments, we showed that during cell infection VP4 interacts with Rab5 and PRA1 proteins. The VP4 domain implicated in both interactions is located between aa 560 and 722. Interaction between VP4 and Rab5 occurs at an early step of

* Corresponding author. Mailing address: Virologie Moléculaire et Structurale, UMR CNRS-INRA 2472, Avenue de la Terrasse, F-91190 Gif-sur-Yvette, France. Phone: 33(0)169823854. Fax: 33(0)169824308. E-mail: cohen@gv.cnrs-gif.fr.

the infection. We showed also that molecules of VP4 interacting with Rab5 and PRA1 were assembled neither in viral particles nor in the heterotrimeric complexes consisting of VP7, VP4, and NSP4.

MATERIALS AND METHODS

***Saccharomyces cerevisiae* two-hybrid screening.** A Matchmaker monkey CV1 cell cDNA library fused with the yeast GAL4 activation domain in plasmid pGAD 10 was purchased from Clontech. The constructs used as bait corresponded to the VP4, VP5*, and VP8* proteins of bovine rotavirus (RF strain). The VP4 bait was prepared by excision from pBS-RF4 (36) and insertion into the *Bam*HI site of plasmid pGBT9 (Clontech) carrying the GAL4 binding domain. For VP5* and VP8* bait, *Bam*HI restriction sites were introduced at 5′ and 3′ ends of VP5* and VP8* cDNA to allow their cloning in pGBT9, and an ATG start codon was added at the 5′ end of VP5* cDNA. Nucleotides were replaced by performing PCR with pBS-RF4 as template and the indicated primers, which contained a *Bam*HI site (underlined) to subclone VP8* (CGCGGATCCGCGA TGGCTTCACTCATTTAT and CGCGGATCCGCGTTACCTTGATACTAT CGA) and VP5* (CGCGGATCCGCG**ATG**AATATTGTATATACA and CGC GGATCCGCGTTACAAGCGACATTGCAT). The added start codon in VP5* is indicated in boldface. Plasmid constructs were referred to as pGAL-VP4, pGAL-VP5*, and pGAL-VP8*. The yeast HF7C strain containing the two reporter genes *his3* and *lacZ* was first transformed with the bait plasmid by a lithium acetate protocol (18). HF7C cells selected for growth in Trp-deficient medium were then transformed with plasmid DNA from a pGAD 10 CV1 cDNA library. The capacity to grow on Leu-deficient medium is provided by pGBT9. Double transformants were grown on plates containing medium lacking Trp and Leu (Trp^- Leu^-) to select for the presence of both the bait and the library plasmids. Additionally they were grown on medium deprived of Trp, Leu, and His (Trp^- Leu^- His^-) to select for protein-protein interactions. Positive clones were then assayed for β-galactosidase activity as instructed by the supplier (Clontech). Plasmid DNA isolated from yeast clones was then transformed into *Escherichia coli* HB101 and sequenced with an ABI 310 sequencer by using pGAD direct and reverse primers. Homology searches were performed on the National Center for Biotechnology Information database with BLAST and PSI-BLAST (3).

Antibodies. Monoclonal antibody (MAb) to the Rab5 protein was purchased from Synaptic System GmbH, Goettingen, Germany. For immunostaining and immunoprecipitation experiments, we used a panel of murine MAbs directed against rotavirus proteins. MAbs 5.73, 1026, and E22 are directed against VP4, VP6, and VP2, respectively (27, 36, 41). A rabbit anti-NSP4 antiserum directed against the C-terminal part of NSP4 was used in immunostaining experiments (kindly supplied by L. Svensson, SMI Stockholm). M5 MAb against the FLAG peptide was purchased from Sigma. A nonrelevant MAb against human kappa light chain, KP-53, was purchased from Sigma and used for controls. Peroxidase-conjugated secondary antibody was purchased from Amersham, Les Ulis, France.

Infection of cultured cells, immunoprecipitation, and Western blotting. Fetal rhesus monkey kidney cell line MA104 was grown to confluent monolayers in Eagle's minimal essential medium (Life Technologies, Paisley, Scotland) supplemented with 10% fetal calf serum and antibiotics. MA104 monolayers were washed with serum-free medium and infected with bovine rotavirus (RF strain) at a multiplicity of infection of 10 PFU/cell. At various times postinfection (p.i.), cells were washed in phosphate-buffered saline, harvested into 10 mM potassium acetate–10 mM HEPES (pH 7.3) containing aprotinin (10 μg/ml) and leupeptin (10 μg/ml), and swelled on ice for 10 min. Cells were then lysed by 10 passages through a 26-gauge needle, and the buffer was adjusted to 25 mM potassium acetate and 125 mM HEPES, pH 7.3. The cellular homogenate was centrifuged at $2,000 \times g$ for 20 min to remove nuclei. Endosomal and cytosolic Rab5 were recovered in the supernatant after centrifugation at $18,600 \times g$ for 15 min. Lysates corresponding to 9×10^6 cells were immunoprecipitated with antibodies for 1 h at 37°C, and then 40 μl of protein A-Sepharose CL-4B beads (Pharmacia) was added to the mixture and incubated for 1 h at room temperature. Beads coupled to immune complexes were washed four times with 25 mM potassium acetate–125 mM HEPES, pH 7.3, buffer, supplemented with aprotinin and leupeptin in the concentrations indicated above. Finally, immune complexes were suspended in 20 μl of Laemmli sample buffer and analyzed by sodium dodecyl sulfate-polyacrylamide gel electrophoresis (SDS-PAGE; 12% polyacrylamide) (28) and Western blotting. Proteins were transferred to polyvinyl difluoride membranes that were incubated sequentially with mouse MAb and peroxidase-conjugated anti-mouse secondary antibody and revealed by enhanced chemiluminescence, as instructed by the manufacturer (Amersham).

Construction of FLAG-Rab5 and FLAG-PRA1: transfection of COS-7 cells. Clones selected from the CV1 cell cDNA library contained full-length cDNAs encoding Rab5a, Rab5c, and PRA1. These inserts were subcloned in frame with the C termini of the FLAG amino acid sequence added to pcDNA3.1 ahead of a *Not*I site (D. Poncet, personal communication). Resulting constructs were referred to as pcDNA-Rab5a, pcDNA-Rab5c, and pcDNA-PRA1, respectively. COS-7 cells were grown to confluent monolayers in Dulbecco's modified Eagle's medium supplemented with 10% fetal calf serum. Cells were then transfected with Lipofectamine reagent (Gibco BRL) according to the manufacturer's instructions. After 3 days, cells were washed and infected at a multiplicity of infection of 10 PFU/cell. Lysates were prepared for immunoprecipitation as described above.

Mutants of VP4 and evaluation of their interactions with Rab5a and PRA1. A series of 10 mutants was constructed by either QuikChange (Stratagene, Amsterdam, The Netherlands) or mutagenic PCR methods with pBS-RF4 plasmid as a template (see Fig. 5). Three of these mutants were designed to alter specifically identified motifs: VP5scFus was mutated in the putative fusion domain (P395D and G400D), VP5scInt was mutated in the putative integrin binding domain (R307I, D308A, and G309V), and VP5scCC was mutated in the coiled-coil domain (F505S, L508V, and I512S). The seven mutants with deletions corresponding to amino acid domains 248 to 577, 458 to 568, 560 to 776, 560 to 722, 614 to 776, 248 to 639, and 283 to 776 were referred to as VP5Δsc1, VP5ve1, VP5ve2, VP5ve3, VP5ve4, VP5sc2, and VP5sc3, respectively. After complete nucleotide sequencing, amplified fragments were digested with *Eco*RI and *Pst*I and introduced in a pGBT9 vector (Clontech) previously digested with the same enzymes. We then investigated the interaction of these mutated proteins with GAL4AD-Rab5a or with GAL4AD-PRA1 in yeast cells. Qualitative and quantitative results were obtained by assessing the ability of yeast to grow in the absence of histidine (Trp^- Leu^- His^-), by the appearance of blue colonies in the presence of X-Gal (5-bromo-4-chloro-3-indolylphosphate), and by assaying the β-galactosidase activity of yeast grown in liquid medium with the LacZ chromogenic substrate ONPG (*o*-nitrophenyl-β-D-galactopyranoside) from Sigma-Aldrich, St. Quentin Fallavier, France.

RESULTS

Identification of cellular partners of VP4. In order to identify potential host cell proteins that interact with the VP4 protein of rotavirus, we used the yeast two-hybrid approach. No transactivation signal was detected when HF7C cells were cotransfected with VP4 cDNA containing bait or prey plasmids and with empty prey or bait plasmids. Yeast cells were cotransformed with one of the bait plasmids corresponding to VP4, VP5*, or VP8* and with the prey plasmids containing the monkey CV1 cell cDNA library. With VP8* as bait, none of 1.1×10^6 transformants isolated were able to activate the transcription of both *HIS3* and *lacZ* reporter genes. Thus, no interaction between VP8* and a cellular partner was detected (Table 1). With VP4 and VP5* as baits, 97 clones (34 for VP4 and 63 for VP5*) grew in the absence of histidine and showed blue colonies in the presence of X-Gal substrate. After restriction analysis and sequencing, 27 clones containing two different full-length open reading frames fused to the activating domain of polymerase II were identified. Twenty-two of these clones encoded a 185-aa protein identified as PRA1, and five clones encoded a 217-aa protein identified as Rab5a (Table 1). The Rab5a isoform was detected with both baits, VP4 and VP5*, while the Rab5c isoform was detected only with the VP5* bait. Genes coding for Rab5 and PRA1 were subcloned in pGBT9 and assayed with VP4 and VP5* genes subcloned into pGAD. Under those conditions, symmetrical to the conditions used for the screen, no interaction was observed since no colonies were able to grow in the absence of histidine. This situation could be

TABLE 1. Screening of the monkey CV1 cell cDNA library with VP4, VP5*, and VP8* proteins of rotavirus

Bait	Transformant[a]	Prey[b]		
		Rab5apGBT9	Rab5cpGBT9	PRA1pGBT9
VP4pGAD[c]	1×10^6	1	0	5
VP5*pGAD	1.2×10^6	3	1	17
VP8*pGAD	1.1×10^6	0	0	0

[a] Number of transformants isolated on the basis of their ability to grow on medium containing histidine.
[b] Number of transformants growing in the absence of histidine and producing blue colonies in the presence of X-Gal substrate (induction of both reporter genes, *his3* and *lacZ*).
[c] Controls for self-activation of the fusion protein (i.e., after cotransfection with VP4, VP5*, and VP8* fused to the activation domain in pGAD and the empty pGBT9) did not show colony growth in the absence of histidine.

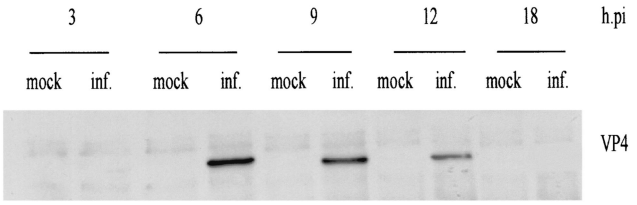

FIG. 2. Time course of interaction between VP4 and Rab5. Lysates were prepared from mock-infected (mock) or infected (inf.) MA104 cells at 3, 6, 9, 12, and 18 h after rotavirus infection. Each lane corresponds to the total protein content of 9×10^6 cells. These lysates were subjected to immunoprecipitation with protein A-Sepharose beads loaded with anti-Rab5 MAb. Immunoprecipitates were analyzed by SDS-PAGE and anti-VP4 Western blotting.

due to the folding of fusion proteins and has been previously observed (22).

Evidence of interaction between VP4 and Rab5. Coimmunoprecipitation studies were performed to determine the association of Rab5 with VP4 in infected cells. Both VP4 and Rab5 can be detected by Western blotting in lysates of MA104 cells infected with bovine rotavirus (Fig. 1A, lanes 1 and 2). Rab5 complexes were immunoprecipitated with anti-Rab5 MAb, and VP4 present in these complexes was detected by immunostaining. Thus, we demonstrated an interaction between VP4 and Rab5 (Fig. 1B, lane 4). The specificity of Rab5 complex immunoprecipitation was also shown by the use of a nonrelevant MAb with which no VP4 was detected (Fig. 1B, lanes 9 and 10). COS-7 cells were separately transfected with plasmids allowing expression of either FLAG-Rab5a or FLAG-Rab5c protein. Transfected cells were then infected with rotavirus. In both cases we detected VP4-Rab5 complexes after immunoprecipitation by an anti-FLAG MAb, which detects only the plasmid-directed expression of Rab5 (isoforms a and c) and not the endogenous molecules. No coimmunoprecipitation of VP4 and Rab5 was observed with the anti-FLAG MAb in lysate from COS-7 cells transfected with an empty plasmid. These results clearly indicated that VP4 interacts specifically with both Rab5a and Rab5c (Fig. 1B, lanes 6 and 8).

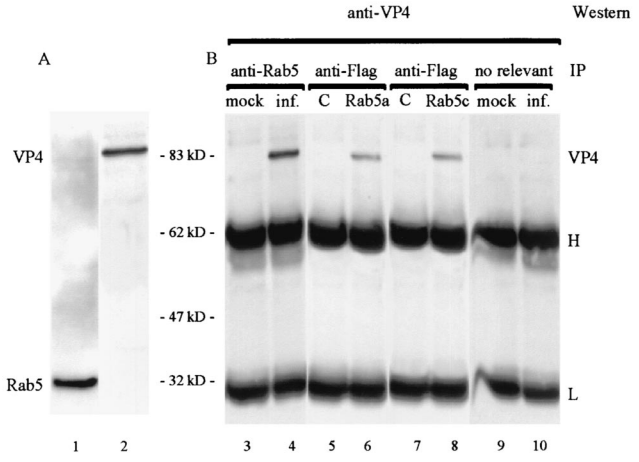

FIG. 1. Coimmunoprecipitation of VP4 and Rab5 protein in infected MA104 and transfected COS-7 cells. (A) Lysate from infected MA104 cells at 6 h p.i. was analyzed by SDS-PAGE and anti-Rab5 or anti-VP4 Western blotting (lanes 1 and 2, respectively). (B) Lysates from infected (inf.) or mock-infected (mock) MA104 cells were subjected to immunoprecipitation with protein A-Sepharose beads loaded with anti-Rab5 MAb (lanes 3 and 4) or nonrelevant antibody (lanes 9 and 10). Immunoprecipitates were analyzed by SDS-PAGE and anti-VP4 Western blotting. Lysates for infected and transfected COS-7 cells with pcDNA3.1-Rab5a (Rab5a), pcDNA3.1-Rab5c (Rab5c), and pcDNA3.1 (C) were subjected to immunoprecipitation with protein A-Sepharose beads loaded with anti-FLAG MAb. Immunoprecipitates were analyzed by SDS-PAGE and anti-VP4 Western blotting. Molecular mass markers are indicated between panels A and B. H and L correspond to heavy and light chains of immunoglobulin G, respectively.

The presence of VP4 implicated in the complexes was monitored during the infection cycle by immunoprecipitation of infected-cell lysates with anti-Rab5 MAb and anti-VP4 immunostaining (Fig. 2). VP4 was detected in association with Rab5 by 6 h p.i. At 18 h p.i., VP4 was no longer detected. The absence of VP4-Rab5 complexes at a late stage of infection could be due to several factors including (i) reduction in the synthesis of Rab5, like that of most cellular proteins during the late stages of infection; (ii) a change in the phosphorylation state of Rab5; (iii) a change in Rab5 localization, cytoplasmic or membrane bound; and (iv) the amount of available free VP4, which is consumed for the final assembly of mature virions.

Rab5 does not interact with VP4 assembled in viral particles nor with heterotrimer NSP4-VP7-VP4. In order to determine whether VP4 interacting with Rab5 was free VP4 or VP4 incorporated into virus particles or heterotrimers previously described (33, 39), we analyzed the complexes immunoprecipitated with anti-Rab5 MAb for the presence of VP6, VP2, and NSP4. As shown in Fig. 3 (lanes 1, 3, 5, and 7), out of the four viral proteins tested, only VP4 was present in complexes containing Rab5. We checked also that these viral proteins were present in cell lysates in sufficient amounts to be detected by immunostaining (Fig. 3, lanes 4, 6, and 8). These results indicated that molecules of VP4 interacting with Rab5 were not found in mature viral particles or in heterotrimeric complexes.

Evidence of interaction between VP4 and PRA1. To confirm results obtained after the two-hybrid screening, we performed immunoprecipitation of complexes containing PRA1. Since no good serum against PRA1 was available, COS-7 cells were transfected with a construct allowing the expression of the FLAG-tagged PRA1 and infected 48 h later by rotavirus. Ly-

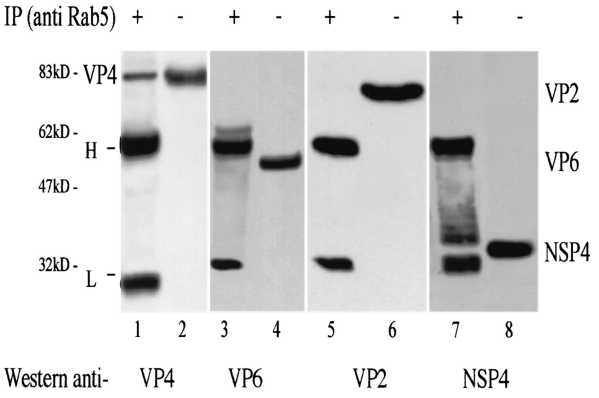

FIG. 3. Interaction among rotavirus proteins VP2, VP6, NSP4, and Rab5. Lysate of infected MA104 cells 6 h p.i. was subjected to immunoprecipitation with protein A-Sepharose beads loaded with anti-Rab5 MAb. Immunoprecipitates were analyzed by SDS-PAGE and anti-VP4, anti-VP6, anti-VP2, or anti-NSP4 Western blotting (lanes 1, 3, 5, and 7, respectively). The same lysates were analyzed directly, i.e., prior to immunoprecipitation, by SDS-PAGE and anti-VP4, anti-VP6, anti-VP2, or anti-NSP4 Western blotting (lanes 2, 4, 6, and 8, respectively). Each lane corresponds to the total protein content of 9×10^6 cells. H and L correspond to heavy and light chains of immunoglobulin G, respectively. The additional band present in lane 7 is probably due to a contaminant protein in the anti-Rab5 antibodies. Migration of molecular mass markers is indicated on the left.

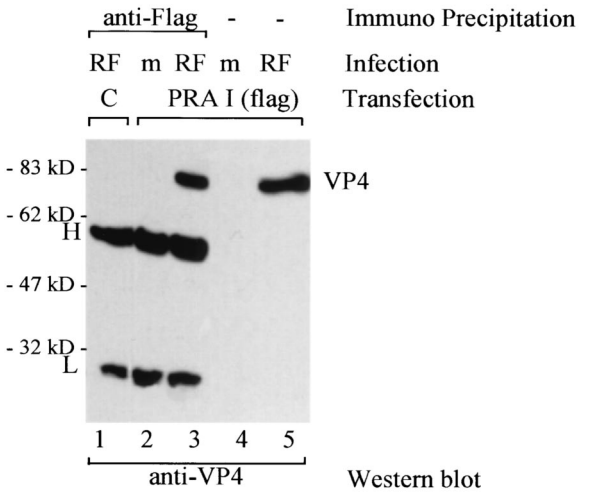

FIG. 4. Interaction between VP4 and PRA1. Lysates from infected (RF) or mock-infected (m) COS-7 cells transfected with pcDNA3.1-PRA1 were subjected to immunoprecipitation with protein A-Sepharose beads loaded with antibodies specific for FLAG. A lysate of infected and transfected COS-7 cells with pcDNA3.1 Hygro-FLAG vector was used as a control and submitted to the same immunoprecipitation procedure (lane 1). Immunoprecipitates were analyzed by SDS-PAGE and anti-VP4 Western blotting. Total lysates from infected (RF) or from mock-infected (m) COS-7 cells transfected with pcDNA3.1-PRA1 were analyzed by SDS-PAGE and anti-VP4 Western blotting (lanes 4 and 5). Each lane corresponds to the total protein content of 9×10^6 cells. H and L correspond to heavy and light chains of immunoglobulin G, respectively. Migration of molecular mass markers is indicated on the left.

sates were prepared 6 h p.i. in the absence of detergent as above and submitted to immunoprecipitation with an anti-FLAG MAb. The presence of VP4 in immune complexes was analyzed by VP4-specific immunostaining. As shown in Fig. 4 (lane 3) and in contrast with mock-infected cells (Fig. 4, lane 2), detection of VP4 was specific for infected cells, thus demonstrating interaction between VP4 and PRA1 during infection. A lysate of infected COS-7 cells transfected with an "empty" plasmid was used as a control (Fig. 4, lane 1).

Identification of VP4 domains involved in binding to Rab5 and to PRA1. VP4 is a 776-aa-long protein that presents four previously described signatures: (i) an amino-terminal trypsin cleavage product, VP8* (13, 17), which carries hemagglutinin activity; (ii) an integrin-interacting domain (aa 308 to 310) (21); (iii) a fusogenic domain (aa 384 to 404) (14); and (iv) a coiled-coil domain (aa 494 to 554) (31). Screening the yeast two-hybrid system clearly showed that VP8* does not interact with PRA1 (Table 1 and Fig. 5). Reproducibly, the interaction between VP4 and Rab5 or PRA1 was stronger when assayed with the VP5* domain than when assayed with the full-length VP4 (Fig. 5, pGAL-VP4 and pGAL-VP5*, respectively). The difference in reactivity between VP4 and VP5* may be related to differences in folding of these proteins as such or, since in the two-hybrid assays they are expressed as fusion proteins, to different folding of the fusion products. Truncated derivatives of VP4 could be misfolded and may not be able to preserve the structure necessary for their ability to interact with partners.

To evaluate the role of the predicted functional domains, we have constructed three site-directed mutants with mutations in the predicted motifs. Mutations have been selected on the basis of the comparisons of the numerous VP5* sequences available and also because they are likely to alter the identified functions of these sites. In addition, in order to grossly identify the domains of VP5* implicated in the interactions with Rab5 and PRA1, seven VP5* proteins with different deletions at the C- and N-terminal ends have been constructed. The readout of the interaction was the growth of yeasts harboring the two plasmids in His^- medium. The interaction of the various VP5* mutants with Rab5a or PRA1 was confirmed in a quantitative galactosidase assay based on the induction of the *lacZ* gene. Wild-type VP5* and VP8* were used as positive and negative controls, respectively. Mutations in two putative functional domains of VP5*, namely, the fusion and integrin receptor domains, reduced but did not suppress the interaction with PRA1 and Rab5. Mutation in the coiled-coil domain did not alter interaction between VP5* and PRA1 but abolished the interaction between VP5* and Rab5. Vice versa, the deletion mutant VP5Δsc2 interacted with Rab5 but not with PRA1. As illustrated in Fig. 5, two deletion mutants of VP5* (VP5Δve2 and VP5Δve3), truncated by 559 aa from the N-terminal end, were able to interact with PRA1 and Rab5. This analysis allowed the conclusion that the same region, extending from residues 560 to 722, is responsible for the binding of VP4 to both Rab5 and PRA1.

DISCUSSION

Rab5 and PRA1 clones were isolated as VP4 and VP5* fused to the activating domain-interacting clones in a yeast two-hybrid screen of a monkey CV1 cell cDNA library. When VP4 and VP5* were fused to the DNA binding domain, no interaction was recorded. Lack of interaction in this situation

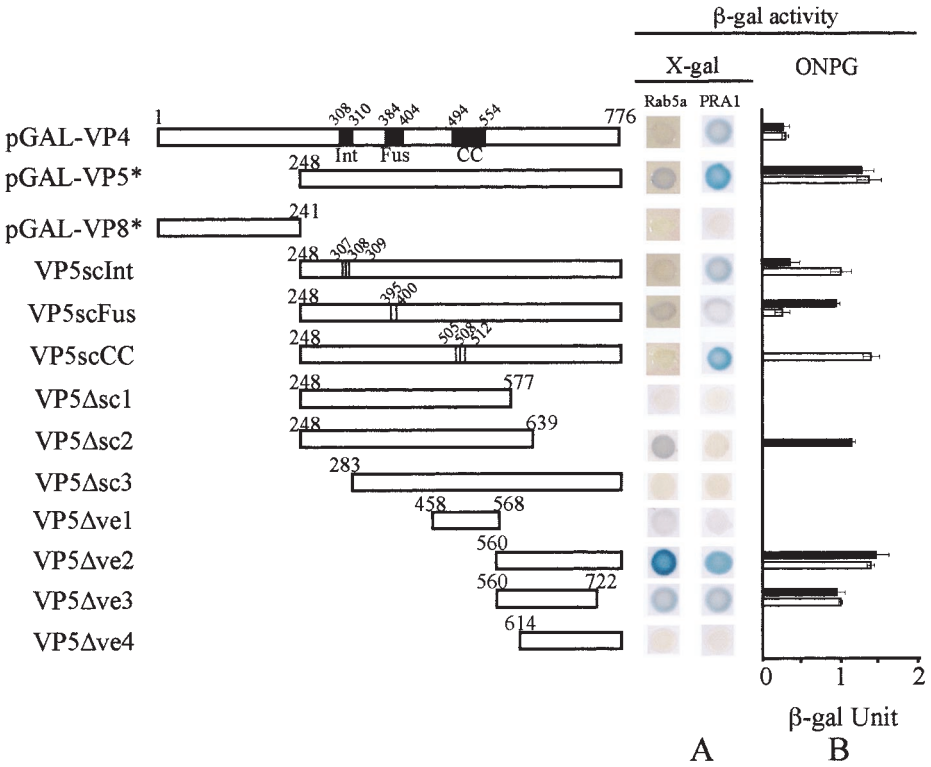

FIG. 5. Schematic diagram of the truncated VP4 and VP5* proteins fused to the GAL4 binding domain and analysis of VP4-Rab5 and VP4-PRA1 interactions. (A) Bars represent the protein product of each deleted VP4 gene, with amino acid positions indicated. Positions of amino acid changes are indicated for VP5scFus, VP5scInt, and VP5scCC mutants. Int, integrin receptor; Fus, fusogen domain; CC, coiled-coil sequence. HF7C yeast was cotransformed with the indicated mutant and pGAD-Rab5a and pGAD-PRA1. The interaction was assessed by checking for blue colonies in the presence of X-Gal. (B) Quantitative evaluations of the interactions were obtained from independent yeast cotransformants assayed with ONPG as substrate. β-Galactosidase activity was expressed in units and calculated by the following formula: $(1{,}000\,A_{420})/(A_{600}TV)$, where A_{420} is the absorbance of the reaction mixture, A_{600} is the cell density of the culture, T is the reaction time (in minutes), and V is the volume (in milliliters) used for the assay. Solid and open bars correspond to interactions of Rab5 and PRA1 with constructs indicated, respectively. Standard deviations are shown ($n = 3$).

was observed by Ito et al. when analyzing a great number of interactions in cells in the dual-hybrid assay (22). Moreover, the presence of a coiled-coil structure has also been reported as an obstacle in two-hybrid assays (37). The coiled-coil domain predicted in VP4 (31) could explain why the detection of the interaction is not symmetrical. The interaction of VP4 with both cellular partners, Rab5 and PRA1, was confirmed by coimmunoprecipitation of infected- or transfected-cell lysates. This interaction occurs at an early step of the infection and disappears before cell lysis. This is most probably due to the decreased amount of Rab5 synthesized after cell infection, due to either its degradation or a decreased Rab5 synthesis. This decreased amount of Rab5 could explain why we did not detect VP4/Rab5 complexes any longer at 18 h p.i. and suggests that the endocytic activity of infected cells could be drastically affected by the infection.

Site-directed mutagenesis in the fusion or in the integrin domain did not suppress the interaction of VP5* with Rab5 and PRA1. By contrast, mutations designed to alter the coiled-coil domain abolished the interaction of VP5* with Rab5, but not with PRA1. On the other hand, the mutant VP5Δsc2, the deletion which extends from residues 248 to 639 of VP4, interacted with Rab5, but no longer with PRA1. Despite a schematic model of the general topology of VP4 and predictions of secondary structure (31, 47), consequences of mutations for the global conformation of VP5* cannot be precisely envisioned, and only mutants that give a positive signal when assayed in the dual-hybrid system have to be considered. A summary of data derived from mutant analysis could be as follows: (i) the domain aa 560 to 722 is necessary for the interaction of VP5 with both partners, and (ii) interactions with Rab5 and PRA1 can be dissociated as evidenced by the two mutants VP5scCC and VP5Δsc2.

Proteins involved in the control of the secretory pathway are often conserved from yeast to mammals (5). Sequence comparisons have indicated that the yeast homologues of Rab5 and PRA1 are Vps21p/Ypt51p and Yip3p, respectively (34, 46). Thus, it is possible that the interactions between VP4 and PRA1 or Rab5 as well as between Rab5 and PRA1 (6), demonstrated in a yeast dual-hybrid screen, were not direct but were mediated through a yeast partner. VP4, PRA1, and Rab5 have been individually expressed in a bacterial expression system. Attempts to confirm the interaction between VP4 or VP5* and Rab5 or PRA1 by glutathione *S*-transferase pull-down assays were unsuccessful (data not shown). These results may suggest that interactions among VP4, PRA1, and Rab5 were indeed not direct and could imply additional molecules.

Adenovirus penton binds to αV integrin, and this interaction

activates the phosphatidylinositol 3-kinase, which in turn regulates endocytosis via Rab5 (40). αV integrins are coreceptors of both rotaviruses and adenoviruses (4, 20). Modes of involvement of Rab5 are quite different in the replication cycles of these different virus families, but this does not imply a participation of Rab5 at distinct steps of the infection. In the case of adenovirus, Rab5 appears to play a role in the entry of virus in early endosomes. The contribution of Rab5 in the rotavirus life cycle is still unclear and needs to be further characterized. The absence of interaction of Rab5 with TLPs and at very early steps of infection (before 6 h p.i.) strongly argues against a role of Rab5 in rotavirus entry. The absence of interaction with the NSP4-VP4-VP7 trimeric complex does not favor a role of Rab5 in the assembly of neovirions, i.e., near the end of the replication cycle. From these results it is likely that VP4-Rab5, VP4-PRA1, and/or VP4-PRA1-Rab5 complexes that could also contain other host proteins are involved in the homeostasis of free cytosolic VP4, whose functions remain to be clarified.

Like rotavirus VP4, the cytoplasmic domain of the structural transmembrane protein gp41 of simian immunodeficiency virus, like that of other phylogenetically diverse lentiviruses, interacts with PRA1 in dual-hybrid experiments (16). PRA1 localizes to Golgi membranes and appears to participate in vesicular trafficking. It has been previously demonstrated that rotavirus and VP4 do not associate with the Golgi apparatus (23, 43). However, it has also been shown that VP4 and complete rotavirus particles strongly associate with lipid raft microdomains that originate from the Golgi apparatus. It is therefore tempting to speculate that an interaction between PRA1 and VP4 may participate in the recruitment of VP4 to these raft membrane domains, a process that will later favor both virus assembly and VP4 expression at the cell surface (36). The association of both gp160 and VP4 with PRA1 is consistent with the demonstration that both viral proteins are found associated with rafts (42, 43), themselves originating from Golgi membranes (8).

ACKNOWLEDGMENTS

We are grateful to D. Poncet for valuable advice in the yeast two-hybrid experiments and for providing Hygro-FLAG plasmid and to C. Jaeger for technical support. We thank U. Desselberger for critical reading of the manuscript and also B. Goud, C. Sapin, and M. Nejmeddine for various suggestions.

REFERENCES

1. **Abdul-Ghani, M., P. Y. Gougeon, D. C. Prosser, L. F. Da-Silva, and J. K. Ngsee.** 2001. PRA isoforms are targeted to distinct membrane compartments. J. Biol. Chem. **276:**6225–6233.
2. **Alory, C., and W. E. Balch.** 2000. Molecular basis for Rab prenylation. J. Cell Biol. **150:**89–103.
3. **Altschul, S. F., T. L. Madden, A. A. Schaffer, J. Zhang, Z. Zhang, W. Miller, and D. J. Lipman.** 1997. Gapped BLAST and PSI-BLAST: a new generation of protein database search programs. Nucleic Acids Res. **25:**3389–3402.
4. **Belin, M. T., and P. Boulanger.** 1993. Involvement of cellular adhesion sequences in the attachment of adenovirus to the HeLa cell surface. J. Gen. Virol. **74:**1485–1497.
5. **Bennett, M. K., and R. H. Scheller.** 1993. The molecular machinery for secretion is conserved from yeast to neurons. Proc. Natl. Acad. Sci. USA **90:**2559–2563.
6. **Bucci, C., M. Chiariello, D. Lattero, M. Maiorano, and C. B. Bruni.** 1999. Interaction cloning and characterization of the cDNA encoding the human prenylated Rab acceptor (PRA1). Biochem. Biophys. Res. Commun. **258:** 657–662.
7. **Chavrier, P., and B. Goud.** 1999. The role of ARF and Rab GTPases in membrane transport. Curr. Opin. Cell Biol. **11:**466–475.
8. **Cheong, K. H., D. Zacchetti, E. E. Schneeberger, and K. Simons.** 1999. VIP17/MAL, a lipid raft-associated protein, is involved in apical transport in MDCK cells. Proc. Natl. Acad. Sci. USA **96:**6241–6248.
9. **Chiariello, M., C. B. Bruni, and C. Bucci.** 1999. The small GTPases Rab5a, Rab5b and Rab5c are differentially phosphorylated in vitro. FEBS Lett. **453:**20–24.
10. **Crawford, S. E., M. Labbe, J. Cohen, M. H. Burroughs, Y. J. Zhou, and M. K. Estes.** 1994. Characterization of virus-like particles produced by the expression of rotavirus capsid proteins in insect cells. J. Virol. **68:**5945–5952.
11. **Crawford, S. E., S. K. Mukherjee, M. K. Estes, J. A. Lawton, A. L. Shaw, R. F. Ramig, and B. V. Prasad.** 2001. Trypsin cleavage stabilizes the rotavirus VP4 spike. J. Virol. **75:**6052–6061.
12. **Denisova, E., W. Dowling, R. LaMonica, R. Shaw, S. Scarlata, F. Ruggeri, and E. R. Mackow.** 1999. Rotavirus capsid protein VP5* permeabilizes membranes. J. Virol. **73:**3147–3153.
13. **Dormitzer, P. R., H. B. Greenberg, and S. C. Harrison.** 2001. Proteolysis of monomeric recombinant rotavirus VP4 yields an oligomeric VP5* core. J. Virol. **75:**7339–7350.
14. **Dowling, W., E. Denisova, R. LaMonica, and E. R. Mackow.** 2000. Selective membrane permeabilization by the rotavirus VP5* protein is abrogated by mutations in an internal hydrophobic domain. J. Virol. **74:**6368–6376.
15. **Estes, M. K.** 2001. Rotaviruses and their replication, p. 1747−1786. *In* D. M. Knipe and P. M. Howley (ed.), Fields virology. Raven Press, Ltd., New York, N.Y.
16. **Evans, D. T., K. C. Tillman, and R. C. Desrosiers.** 2002. Envelope glycoprotein cytoplasmic domains from diverse lentiviruses interact with the prenylated Rab acceptor. J. Virol. **76:**327–337.
17. **Fiore, L., H. B. Greenberg, and E. R. Mackow.** 1991. The VP8 fragment of VP4 is the rhesus rotavirus hemagglutinin. Virology **181:**553–563.
18. **Gietz, D., A. St. Jean, R. A. Woods, and R. H. Schiestl.** 1992. Improved method for high efficiency transformation of intact yeast cells. Nucleic Acids Res. **20:**1425.
19. **Gorvel, J. P., P. Chavrier, M. Zerial, and J. Gruenberg.** 1991. Rab5 controls early endosome fusion in vitro. Cell **64:**915–925.
20. **Guerrero, C. A., E. Mendez, S. Zarate, P. Isa, S. Lopez, and C. F. Arias.** 2000. Integrin α(v)β(3) mediates rotavirus cell entry. Proc. Natl. Acad. Sci. USA **97:**14644–14649.
21. **Hewish, M. J., Y. Takada, and B. S. Coulson.** 2000. Integrins α2β1 and α4β1 can mediate SA11 rotavirus attachment and entry into cells. J. Virol. **74:** 228–236.
22. **Ito, T., K. Tashiro, S. Muta, R. Ozawa, T. Chiba, M. Nishizawa, K. Yamamoto, S. Kuhara, and Y. Sakaki.** 2000. Toward a protein-protein interaction map of the budding yeast: a comprehensive system to examine two-hybrid interactions in all possible combinations between the yeast proteins. Proc. Natl. Acad. Sci. USA **97:**1143–1147.
23. **Jourdan, N., M. Maurice, D. Delautier, A. M. Quero, A. L. Servin, and G. Trugnan.** 1997. Rotavirus is released from the apical surface of cultured human intestinal cells through nonconventional vesicular transport that bypasses the Golgi apparatus. J. Virol. **71:**8268–8278.
24. **Kapikian, A. Z.** 1996. Overview of viral gastroenteritis. Arch. Virol. Suppl. **12:**7–19.
25. **Karcher, R. L., S. W. Deacon, and V. I. Gelfand.** 2002. Motor-cargo interactions: the key to transport specificity. Trends Cell Biol. **12:**21–27.
26. **Kirkwood, C. D., R. F. Bishop, and B. S. Coulson.** 1998. Attachment and growth of human rotaviruses RV-3 and S12/85 in Caco-2 cells depend on VP4. J. Virol. **72:**9348–9352.
27. **Kohli, E., L. Maurice, C. Bourgeois, J. B. Bour, and P. Pothier.** 1993. Epitope mapping of the major inner capsid protein of group A rotavirus using peptide synthesis. Virology **194:**110–116.
28. **Laemmli, U. K.** 1970. Cleavage of structural proteins during the assembly of the head of bacteriophage T4. Nature **227:**680–685.
29. **Li, G., M. A. Barbieri, M. I. Colombo, and P. D. Stahl.** 1994. Structural features of the GTP-binding defective Rab5 mutants required for their inhibitory activity on endocytosis. J. Biol. Chem. **269:**14631–14635.
30. **Lopez, S., C. F. Arias, J. R. Bell, J. H. Strauss, and R. T. Espejo.** 1985. Primary structure of the cleavage site associated with trypsin enhancement of rotavirus SA11 infectivity. Virology **144:**11–19.
31. **Lopez, S., I. Lopez, P. Romero, E. Mendez, X. Soberon, and C. F. Arias.** 1991. Rotavirus YM gene 4: analysis of its deduced amino acid sequence and prediction of the secondary structure of the VP4 protein. J. Virol. **65:**3738–3745.
32. **Ludert, J. E., N. Feng, J. H. Yu, R. L. Broome, Y. Hoshino, and H. B. Greenberg.** 1996. Genetic mapping indicates that VP4 is the rotavirus cell attachment protein in vitro and in vivo. J. Virol. **70:**487–493.
33. **Maass, D. R., and P. H. Atkinson.** 1990. Rotavirus proteins VP7, NS28, and VP4 form oligomeric structures. J. Virol. **64:**2632–2641.
34. **Martincic, I., M. E. Peralta, and J. K. Ngsee.** 1997. Isolation and characterization of a dual prenylated Rab and VAMP2 receptor. J. Biol. Chem. **272:**26991–26998.
35. **McLauchlan, H., J. Newell, N. Morrice, A. Osborne, M. West, and E. Smythe.** 1998. A novel role for Rab5-GDI in ligand sequestration into clathrin-coated pits. Curr. Biol. **8:**34–45.

36. **Nejmeddine, M., G. Trugnan, C. Sapin, E. Kohli, L. Svensson, S. Lopez, and J. Cohen.** 2000. Rotavirus spike protein VP4 is present at the plasma membrane and is associated with microtubules in infected cells. J. Virol. **74:**3313–3320.
37. **Newman, J. R., E. Wolf, and P. S. Kim.** 2000. A computationally directed screen identifying interacting coiled coils from *Saccharomyces cerevisiae*. Proc. Natl. Acad. Sci. USA **97:**13203–13208.
38. **Nielsen, E., F. Severin, J. M. Backer, A. A. Hyman, and M. Zerial.** 1999. Rab5 regulates motility of early endosomes on microtubules. Nat. Cell Biol. **1:**376–382.
39. **Poruchynsky, M. S., D. R. Maass, and P. H. Atkinson.** 1991. Calcium depletion blocks the maturation of rotavirus by altering the oligomerization of virus-encoded proteins in the ER. J. Cell Biol. **114:**651–656.
40. **Rauma, T., J. Tuukkanen, J. M. Bergelson, G. Denning, and T. Hautala.** 1999. Rab5 GTPase regulates adenovirus endocytosis. J. Virol. **73:**9664–9668.
41. **Roseto, A., R. Scherrer, J. Cohen, M. C. Guillemin, A. Charpilienne, C. Feynerol, and J. Peries.** 1983. Isolation and characterization of anti-rotavirus immunoglobulins secreted by cloned hybridoma cell lines. J. Gen. Virol. **64:**237–240.
42. **Rousso, I., M. B. Mixon, B. K. Chen, and P. S. Kim.** 2000. Palmitoylation of the HIV-1 envelope glycoprotein is critical for viral infectivity. Proc. Natl. Acad. Sci. USA **97:**13523–13525.
43. **Sapin, C., O. Colard, O. Delmas, C. Tessier, M. Breton, V. Enouf, S. Chwetzoff, J. Ouanich, J. Cohen, C. Wolf, and G. Trugnan.** 2002. Rafts promote assembly and atypical targeting of a nonenveloped virus, rotavirus, in Caco-2 cells. J. Virol. **76:**4591–4602.
44. **Schalk, I., K. Zeng, S. K. Wu, E. A. Stura, J. Matteson, M. Huang, A. Tandon, I. A. Wilson, and W. E. Balch.** 1996. Structure and mutational analysis of Rab GDP-dissociation inhibitor. Nature **381:**42–48.
45. **Shaw, A. L., R. Rothnagel, C. Q. Zeng, J. A. Lawton, R. F. Ramig, M. K. Estes, and B. V. Prasad.** 1996. Rotavirus structure: interactions between the structural proteins. Arch. Virol. Suppl. **12:**21–27.
46. **Singer-Kruger, B., H. Stenmark, and M. Zerial.** 1995. Yeast Ypt51p and mammalian Rab5: counterparts with similar function in the early endocytic pathway. J. Cell Sci. **108:**3509–3521.
47. **Tihova, M., K. A. Dryden, A. R. Bellamy, H. B. Greenberg, and M. Yeager.** 2001. Localization of membrane permeabilization and receptor binding sites on the VP4 hemagglutinin of rotavirus: implications for cell entry. J. Mol. Biol. **314:**985–992.